

1 **Understanding shallow landslides in Campos do Jordão Municipality**  
2 **– Brazil: disentangle the anthropic effects from natural causes in the**  
3 **disaster of 2000**

4 Rodolfo M. Mendes<sup>1</sup>, Márcio Roberto M. de Andrade<sup>1</sup>, Javier Tomasella<sup>1</sup>, Márcio Augusto E. de  
5 Moraes<sup>1</sup>, Graziela B. Scofield<sup>1</sup>

6 <sup>1</sup>National Center for Monitoring and Early Warning of Natural Disasters, Parque Tecnológico/São José dos Campos, Estrada  
7 Doutor Altino Bondesan 500,12247-016, São Paulo, Brazil

8 *Correspondence to:* Rodolfo M. Mendes (rodolfo.mendes@cemaden.gov.br)

9 **Abstract.** Located in a mountain area of Southeast Brazil, the municipality of Campos do Jordão has been hit by several  
10 landslides in recent history. Among those events, the landslides of early 2000 were significant for the number of deaths (10),  
11 the population affected and the destruction of infrastructure that caused. The purpose of this study is to assess the relative  
12 contribution of natural and human factors in triggering the landslides of the 2000 event. To achieve this goal, a detailed  
13 geotechnical survey was conducted in three representative slopes of the area to obtain geotechnical parameters needed for  
14 slope stability analysis. Then, a set of numerical experiment with Geo-Slope software was designed including natural and  
15 anthropic factors separately. Results showed that natural factors, thus is, high intensity rainfall and geotechnical conditions,  
16 were not severe enough to trigger landslides in the study area and that human disturbance were entirely responsible for the  
17 landslides events of 2000. Since the anthropic effects used in the simulations are typical of Brazilian hazardous urban areas,  
18 we concluded that the implementation of public policies that constrain the occupation of landslide susceptible areas are  
19 urgently needed.

20 **1 Introduction**

21 Due to the combination of frequent heavy rain of high intensities on landscapes dominated by narrow valley and steep  
22 slopes, large areas of the southeast and south of Brazil are naturally susceptible to landslides. In addition, recent studies by  
23 CEPED (2012) indicates that more than 160 million inhabitants live in urban areas (about 90% of Brazilian population), and  
24 that increased urbanization in cities without urban planning and consequent occupation into hazardous areas have led to the  
25 increasing of this natural disaster~~In addition, population growth, increased urbanization, recent estimations (CEPED 2012)~~  
26 ~~indicates that more than 160 million inhabitants live in urban areas (about 90% of Brazilian population), and expansion of~~  
27 ~~urban construction into hazardous areas have led to an escalating impact of this natural disaster.~~ Consequently, landslides are  
28 directly associated with loss of lives, property and infrastructure damage, and environmental destruction. During 2011, for

29 instance, mountainous regions of Rio de Janeiro State suffered several landslides that caused more than 1,500 deaths and  
30 severe damage to the urban and rural infrastructures (Coelho Netto et al., 2013).

31 In spite of floods (generally gradual flooding) being the most disrupted natural disasters in terms of economic damages and  
32 population affected, landslides have been considered the most severe in terms of dead toll (Londe et al., 2014). Although  
33 landslide and flashfloods usually affect heavily urbanized downtown areas, it is also recognize that poor population living in  
34 the outskirts are more vulnerable to these types of disaster. Increased landslide hazard, for instance, has been related to the  
35 improper cut-and-fill construction of self-built housing on steep slopes, after the removal of vegetation. In addition, because  
36 of the lack of collection systems, sewage is disposed into the hillslope soils further increasing the risks of triggering  
37 landslides, not to mention the health risks associated with the lack of sanitation.

38 Among those areas affected by landslides in SE Brazil, the municipality of Campos do Jordão has been hit by several events  
39 since the seventies. The most recently severe landslides occurred in the early days of 2000, leaving 103 people injured, 10  
40 fatalities, and more than 423 houses at risk of collapse (Londe et al., 2014).

41 Early warning system used by the civil defense in Campos do Jordão and by CEMADEN (National Center for Monitoring  
42 and Early Warning of Natural Disasters) are based on threshold values of 72 h accumulated rainfall, derived from empirical  
43 studies (Tatizana et al., 1987; Santoro et al., 2010). In 2000, rainfall was monitored every 24 h at 7:00 am using manual rain-  
44 gauges, and the threshold value for triggering landslides were based on previous studies in other areas of Brazil. Since the  
45 accumulated rainfall values responsible for the occurrence of the landslides of 2000 were well below the critical line  
46 proposed in previous studies (Tatizana et al., 1987), it was not possible to conduct the pre-emptive evacuation of many  
47 hazardous areas.

48 Although empirical rainfall thresholds are successfully used in operational warning systems to predict shallow landslides  
49 (Lagomarsino et al., 2013), critical rainfall thresholds for triggering landslides vary due to regional and local precipitation  
50 distribution, slope morphometry, soil characteristics, lithology, microclimate and geological history (Crosta, 1998; Van Asch  
51 et al., 1999). Therefore, the reliability of empirically derived critical rainfall threshold depends entirely on the availability of  
52 a significant number of cases relating the occurrence of landslides and rainfall conditions. In this sense, Guzzetti et al. (2007)  
53 lists as regional thresholds those covering regions with a few to many thousands square kilometers and having similar  
54 meteorological, climatic and physiographic characteristics, whereas for local conditions the geomorphology and climate  
55 regime are considered to be applicable to areas that range in the order of hundreds of square kilometers.

56 After the event of 2000, new critical 72 h rainfall thresholds values for landslides were proposed for the area. In addition, the  
57 Civil Defense of the State of São Paulo established new critical rainfall amounts for visually monitoring critical areas in  
58 order to detect early signals that may indicate the imminence of a landslide. However, the peak rainfall intensities recorded  
59 in the event of 2000 did not repeat even since, while irregular occupations continued in many landslide prone areas.  
60 Therefore, a detailed study of the event of 2000 is relevant not only because it's extreme characteristics, but also with the  
61 perspective that memory of the 2000 event is dim and its impacts is largely underestimated among many local residents.

62 In this context, for a limited number of data hydrologic models are relevant for investigating precipitation induced shallow  
63 planar landslides (Terlien, 1998).

64 Given the lack of detailed data from historical landslides events in the municipality of Campos do Jordão, the aim of this  
65 study was to understand the factors responsible for triggering the landslides of early 2000 in the area using a numerical  
66 model that fully couple slope stability analysis with saturated/unsaturated transient pore-water pressure simulations.

67 Physical-based hydrological models have been widely applied to predict pore-pressure build-up due to the infiltration in  
68 shallow landslides (Frattini et al., 2009; Iverson, 2000). Several models, based on the infinite slope concepts, that integrates  
69 hillslope hydrology with slope stability, are reported in literature: for instance SINMAP (Pack et al, 1998), SHALSTAB  
70 (Dietrich et al., 1998), TRIGRS (Baum et al., 2002) and GEOTop-FS (Rigon et al., 2006).

71 During the last decade, physically based landslide prediction models have also been successfully used in early warning  
72 systems. Models used in such applications include, among others, the Combined Hydrology and Stability Model-CHASM  
73 (Thiebes et al, 2014), the High Resolution Slope Stability Simulator ~~-HIRESS HIRELESS-~~ (Rossi et al, 2013); the Slope-  
74 Infiltration Distributed Equilibrium-SLIDE (Liao et al, 2010; Montrasio and Valentino, 2008), the Shallow Landslides  
75 Instability Prediction-SLIP (Montrasio 2000; Montrasio et al, 2011). Another slope stability model is the modular software  
76 package GeoStudio (2012), in which SEEP/W and SLOPE/W plugins are used to simulate the instability of slopes during  
77 extreme rainfalls. Although GeoSlope is a simplified "single slope" model, it has been used in several previous studies to  
78 understand the effect of infiltration on rainfall-induced landslides (for instance Ng and Shi, 1998; Gasmol et al., 2000; Kim et  
79 al., 2004; Huat et al., 2006; Oh and Vanapalli, 2010; Acharya et al., 2016), producing very good results (Tofani et al., 2006).

80 In this study, we analyzed several scenarios that included the relative influence of natural and anthropic factors that prevails  
81 in the area, and identified the most critical factors responsible for the severe landslides of 2000 using the GeoStudio (2012)  
82 software due to its versatility of for handling natural and anthropic boundary conditions separately.

83 In addition, we analyzed if the threshold rainfall values establish by the Civil Defense are adequate for early warning of  
84 landslides occurrence taking into account the today's occupation patterns of landslide prone areas.

85

## 86 **2 Material and Methods**

### 87 **2.1 Study site**

88 The study site is the municipality of Campos do Jordão, of the State of São Paulo, located in a mountainous region along the  
89 Mantiqueira Hills (Figure 1). In geological and geomorphological terms, the Campos do Jordão plateau is a crystalline  
90 plateau block with elevations of more than 2,000 m above sea level and bordered by steep cliffs that rise approximately  
91 1,500 m over the adjacent Paraíba valley (Almeida, 1976). The relief, strongly conditioned by the structures and lithologies  
92 of the area, is characterized by the presence of high hills and erosion of grandstands. On the basis of these amphitheatres  
93 occur peat depressions (Modenesi-Gauttieri and Hiruma, 2004), where deposits of organic clay of varying thickness are

94 found. The geological and geotechnical characteristics of the deposits of organic clay and its quite sensitive behavior to  
95 sudden human interventions that alter their original equilibrium conditions have conditioned the slopes stability in the urban  
96 area of the municipality of Campos do Jordão (Ogura et al., 2004).

97 The area where Campos do Jordão is located was occupied by Portuguese settlers during the XVIII century. During the  
98 hygienist movement (late XIX and early XX centuries), various health facilities were established in the town, mainly for  
99 tuberculosis treatment. Since 1940, the town experienced a large population growth and urban expansion due to the  
100 development of tourism: the number of inhabitants increased from 13 thousand in 1950 to more than 50 thousand according  
101 to the estimates, with density of 164.76 pop/Km<sup>2</sup>, 99.3% of which live in the urban area (IBGE, 2016).

102 The process of accelerated urbanization, specially from the 70s, of areas with unfavorable geotechnical characteristics, has  
103 been pointed out as responsible for most of the natural disasters in Campos do Jordão (Ridente et al., 2002). Table 1 shows  
104 the most important events in terms of dead toll and damages recorded in the area.

105 Landslides in the study area are classified as shallow, translational type, with depths of the rupture surfaces less than 2 m.  
106 Depending on the position of the rupture, three different processes are observed: the rupture surface occurs in the residual  
107 soil of undisturbed ground; the rupture surface occurs in the residual soil of a slope cut; and the rupture surface occurs in the  
108 base of the landfill deposit, or in the slope residual soil with mobilization of the overlying landfill. The last landslide types  
109 are more harmful since they mobilized larger amounts of material. In the case of the event of 2000 (Figure 2), which is the  
110 focus of this study, rainfall began on 31/12/1999, and continued almost uninterrupted for 4 days with high intensity rainfall  
111 bursts. According to the Brazilian Center for Weather forecasting and Climate Study – CPTEC, daily rainfall from  
112 31/12/1999 through 05/01/2000 was, respectively, 78.5, 101, 120, 60, 144.5 and 10.5 mm (Ridente et al., 2002). Landslides  
113 associated with this event, were considered to be one of the most severe in urban areas in Brazil, since hundred of landslides  
114 occurred, mostly in slopes in poor neighborhoods where houses are constructed over cut-and-fill areas.

115 Based on the landslides events of 1972, 1991 and 2000, Ridente et al. (2002) proposed an approximation of the critical  
116 rainfall necessary for the deflagration of landslides in Campos do Jordão, revealing that, in most cases, landslides are due to  
117 occur after three-day rainfalls of about 200 mm, with a daily rainfall of at least 70 mm during the last day analysed. The  
118 Civil Defense Preventive Plan of the State of São Paulo uses three indexes of precipitation accumulated in three days (60, 80  
119 and 100 mm) as critical thresholds to enter into warning level (Santoro et al., 2010). These thresholds were based on the  
120 studies carried out by Tatizana et al. (1987) and has been considered a critical value for issuing early warnings based on  
121 rainfall observation and forecasting.

122 Aiming to develop relationships for the prediction of mass movements in the area, Ahrendt (2005) attempted to correlate  
123 precipitation with the occurrence of landslides based on the critical intensity curves obtained by Tatizana et al. (1987) for  
124 Serra do Mar in the municipality of Cubatão, and by D'Orsi (1997) for Serra da Mantiqueira in the Municipality of Rio de  
125 Janeiro. Results showed that the occurrences of Campos do Jordão were below the critical lines of those areas, indicating  
126 that the rainfall intensities required for triggering landslides in Campos do Jordão are much lower if compared to the other

127 sites. Therefore, the study of Ahrendt (2005) concluded that rainfall characteristics that triggers landslides in Campos do  
128 Jordão are very unique and a different and more detailed approach was needed.

129 Considering the limited historical data of landslide occurrences and the few previous studies in the area that makes extremely  
130 difficult to define accurate critical threshold rainfall values that triggers landslides, in particularly, the effects the  
131 accumulated rainfall on the water movement and its relationship to rapid mass movements.

132 The Brazilian National Centre for Monitoring and Early Warnings of Natural Disasters – CEMADEN began to monitor  
133 Campos do Jordão by the summer of 2012. Most of the occurrences were observed in cut-and-fill slopes, with evident  
134 contribution of wastewater and micro drainage deficiency. Recent history did not recorded occurrences of great magnitude;  
135 however, the destruction, or even the prohibition of occupying damaged houses, is a recurrent problem.

136

## 137 **2.2 Soil moisture monitoring**

138 Soil moisture was monitored in every hourly interval to a depth 3.0 meters along the 12 months (01/01/2016 to 12/31/2016),  
139 using two EnviroScan™ probes installed next of the borehole SD-03 (Figure 3). EnviroScan™ probes are installed into  
140 customized access tubes manufactured by Sentek Pty. Ltd. Inside of the EnviroScan™ probe were distributed six Sentek  
141 capacitance sensor. The capacitance sensor gives an output in volumetric water content (mm of water per 100 mm of soil  
142 measured). This is converted from a scaled frequency reading using a default calibration equation, which is based on data  
143 obtained from numerous scientific studies in a range of soil textures.

144 Before a Sentek capacitance sensor can be installed in the soil, it must have minimum and maximum values set. This is done  
145 using air and water around each sensor (lecture limits of the volumetric water content – dry and saturated, respectively).

146 Soil moisture was monitored during 2016 at hourly intervals and to a depth of 3.0 m using two EnviroScan™ (Campbell  
147 Scientific, 2016) probes installed next of the borehole SD-03 (Figure 2). Each probe included six capacitance sensors that  
148 measured soil moisture every 0.5 m, thus is, at the depths of 0.5, 1.0, until 3.0 m deep, which allowed to monitor moisture  
149 variations of the landfill, residual and saprolite layers. Before the EnviroScan™ capacitance probes were installed in the  
150 soil, maximum and minimum values were normalized by matching the raw readings from each sensor at both 0% (held in  
151 air) and 100% water levels (submerged in water).

## 152 **2.3 Geotechnical survey**

153 SPT (Standard Penetration Test) boreholes were drilled along three profiles of the study site (A-A'; B-B'; C-C' in Figure 3) at  
154 six different positions along the slopes (SD-01 to SD-6, Figure 4). Disturbed and undisturbed samples were taken from the  
155 boreholes for the determination of the parameters used for stability analysis.

156 Three (03) undisturbed samples were collected in migmatitic saprolite block close to the SD-04 borehole. This material  
157 occurs anisotropically and discontinuously, because it presents significant textural variation resulting from the heterogeneity  
158 of the parental rock, being predominantly formed by silt and fine sand, with variable occurrence of clay. From the 6

159 boreholes (SD-1 to SD-6) and the 3 undisturbed blocks it was possible to obtain a total of 12 soil samples to perform  
160 geotechnical characterization tests of the study area following Brazilian standard procedure.

161 Disturbed and undisturbed samples collected were used to perform grain size analysis test (ABNT, 1984b and 1995), soil  
162 particle density (ABNT, 1984a), bulk density, specific dry mass and Atterberg limits (ABNT, 1984c and 1984d). Parameters  
163 of effective cohesion ( $c'$ ) and effective friction angle ( $\phi'$ ) were obtained from saturated direct shear tests, using square  
164 shaped undisturbed samples with 60 mm of side and height of 25 mm. The soil samples were in their natural state, being  
165 representative of the “Residual” and “Saprolite” soil layers. During the consolidation step, all specimens were saturated for  
166 24h and subjected to net normal stresses of 25, 50 and 100 kPa. Then, in the shearing phase, a constant velocity of 0.033 mm  
167  $\text{min}^{-1}$  was applied. Vertical and horizontal displacements were recorded during the consolidation and shearing phases.

168 After saturation soil samples for 12 hours, Water Retention Curves - WRC of the residual soils layers were obtained using  
169 pressure plate for suctions  $<100$  kPa and filter paper for suctions  $\geq 100$  kPa for the drying path of the samples following the  
170 recommendation of Marinho and Oliveira (2006). Results showed that the differences of water retention values at the  
171 transition among both method were not significant, making unnecessary further adjustments (Figure 8). The saturated  
172 hydraulic conductivity -  $K_{\text{sat}}$  was obtained in laboratory using a constant head permeameter. Hydraulic conductivity  
173 functions were estimated from the WRC,  $K_{\text{sat}}$  using the Van Genuchten (1980) model. In the case of landfill deposits, the  
174 values of  $K_{\text{sat}}$  for different soil texture were those obtained Ahrendt (2005) from core measurements.

175

#### 176 **2.4 Modelling experiments**

177 The modelling of the stability and seepage analysis was divided in two parts: (1) transient unsaturated seepage analysis; (2)  
178 stability analyses coupled with the results from the previous step.

179 For the seepage analysis, 35-days accumulated rainfall of the period 01/12/1999 through 04/01/2000 was considered, since  
180 that event triggered several landslides in the study area (Ahrendt and Zuquette, 2003). In addition to the geotechnical  
181 parameters, anthropic factors that induce landslides typical of Brazilian urban slopes, specifically housing load, man-made  
182 cuts and leakage from pipes, were included in the modelling experiment with the aim of analysing the degree of influence of  
183 these factors on the trigger of landslides in the study area during 2000 (Figures 4, 5 and 6).

184 The boundary conditions were set according to field observations on the landslide area and boundary conditions used by  
185 Rahardjo et al. (2007). The non-saturated transient flux results were obtained for two cases: considering only the  
186 accumulated rainfall and rainfall including linear leakage along the cut slope (Figure 5). The initial pore-pressure values used  
187 in the transient flow analysis were obtained indirectly from the WRC and the data of the soil moisture sensors installed in the  
188 study area (Figures 8 and 7). Next, the factor of safety (FS) for the slope was estimated from the transient seepage modelling  
189 coupled with the stability analysis tool (Geo-Slope, 2012a). All the stability analyses were conducted considering the theory  
190 of static equilibrium of forces and momentum. The FS were calculated using the geotechnical and anthropic parameters,  
191 obtained from the method of Morgenstern-Price, which considers circular and non-circular rupture surfaces. All the

192 simulations allowed the slope stability module SLOPE/W to identify the most critical rupture surface (Figure 6). Therefore,  
193 the values of the Slope Safety Factor – FS, were the lowest of all conditions analysed.

194

### 195 **3 Results**

#### 196 **3.1 Geotechnical survey**

197 The result of the granulometric analyses of the residual and saprolite layers of the three profiles studied are presented in  
198 Figure 7. Residual layer (sample SD-01/2.0 m) can be classified as clayey sand, with percentage of sand and silt of 53 % and  
199 25 %, respectively. The soil samples representative of the saprolite layer showed a significant variation of the percentage of  
200 the clay fraction (3 to 24%), silt (14 to 42%) and sand (53 to 73%), indicating that soil profiles are heterogeneous, which in  
201 agreement with the textural characteristics of its parent material (migmatitic gneiss). Therefore, it is expected that the  
202 mechanical and hydraulic properties of this soil layer present high variability. The general results of the geotechnical tests  
203 (general characteristics, shear strength and saturated hydraulic conductivity) of the samples of the representative soils of the  
204 studied area are presented in Table 2.

205 Analysing the values of the effective strength parameters ( $c'$  and  $\phi'$ ) and saturated hydraulic conductivity (Table 2), the  
206 values representative of the 'Saprolite' layer showed significant variability: the coefficient of variation was 85% for the  
207 effective cohesion; 20% for the effective friction angle, and 89% for the saturated hydraulic conductivity, reflecting the  
208 heterogeneity character of the parent material. The high values of the resistance parameters shown in Table 2 can be  
209 explained are associated with the high heterogeneity of the residual gneiss soil, such as the presence quartz particles and  
210 other minerals of considerable size in the specimens tested, which confer them high resistance. In addition, the values of the  
211 resistance and Ksat parameters obtained in this study are close to mean reference values of residual gneiss soils  
212 representative of other Brazilian sites (Costa Filho and Campos, 1991; Ahrendt, 2005; Reis et al., 2011).

213 Figure 8 shows the water retention curves of the soil layers representative of the profiles. In general, the residual and  
214 saprolite layers are able to hold more water compared to the landfill deposit. For example, for a field matrix suction level of  
215 100 kPa, the volumetric moisture values of the Landfill Deposit, Residual Soil and Saprolite layers are, respectively, 0,06  
216  $\text{m}^3/\text{m}^3$ ; 0,24  $\text{m}^3/\text{m}^3$ ; 0,26  $\text{m}^3/\text{m}^3$ .

217

#### 218 **3.2 Soil moisture data**

219 Soil moisture data from 2016 from the EnviroScan™ probes (3G1 and 3G2) are presented in Figure 9. The data from 3G1  
220 (upper graph of Figure 9) showed that the sensor installed at a lower depth (0.5 to 1.0 meter), representative of the landfill  
221 deposit (green curve) layer, have variations larger soil moisture variations ( $\Delta\theta = 32\%$ ), with maximum and minimum water  
222 content values recorded in March (46%) and April (14%), respectively. At deeper layers (1-3 meters deep), representative of  
223 the "Residual" and "Saprolite" layers (black and red curves), time variation of soil moisture is much lower ( $\Delta\theta = 10\%$ , on

224 average). In the Residual layer (black curve), maximum and minimum values of soil moisture were verified in January  
225 (38%) and May (27%), respectively. In the case of the saprolite layer (red curve) maximum and minimum humidity values in  
226 the months of June (40%) and May (32%). The different dynamics among the three soil layers are reflecting not only  
227 differences in the retention properties of each layer considered but also the deep soil water dynamics down the soil profiles.  
228 This explains why the upper layer (landfill deposit) shows a more spiky behaviour in response the rainfall; while the other  
229 two layers exhibit gradual and delayed variations related to deep water percolation.  
230 Analysing the data of the probe 3G2 (lower graph of Figure 9), it is clear that the soil moisture variation of the sensor of the  
231 surface layer, representative of the Landfill Deposit layer (green curve), was significantly lower ( $\Delta\theta = 15\%$ ) compared to the  
232 same layer of probe 3G1. Maximum and minimum soil moisture values were recorded in September (43%) and August  
233 (28%), respectively. At deeper depth, within the residual and saprolite layers (black and red curves), time variation of soil  
234 moisture variation is similar than the measurements of probe 3G1 ( $\Delta\theta = 9\%$ , on average). For the "Residual" layer (black  
235 curve) maximum and minimum soil moisture values were observed in January (31%) and May (21 %), respectively; while in  
236 the "Saprolite" layer (red curve) maximum and minimum soil moisture values in the months of January (37%) and August  
237 (30%).  
238 Contrasting differences in the soil moisture behaviour of the landfill deposit from the probes 3G1 and 3G2 suggest that the  
239 variability of soil parameters is higher in the top layer. This was expected considering that this layer is the result of the cut-  
240 and-fill processes mixed with construction wastes of several types.

### 241 **3.3 GeoSlope simulations input data**

242 Table 3 summarizes the parameters used in the numerical simulation with GeoSlope software, based on the geotechnical  
243 survey and information extracted from different sources.  
244 Regarding the geotechnical properties, in order to reduce the uncertainties due to the heterogeneity of the parent material, the  
245 mean values of the resistance ( $c'$  and  $\phi'$ ), bulk density and saturated hydraulic conductivity parameters for saprolite and  
246 residual (Table 2) were used in the flow and stability modelling. As mentioned before, for the landfill deposit, the  
247 geotechnical parameters were those obtained by Ahrendt (2005).  
248 Based on the field information from previous studies in Brazil, the anthropic factors considered in the simulations were:  
249 point leakage sources of  $1.0 \text{ m}^3\text{day}^{-1}$  (SABESP, 1993 and 2016) for simulation that include leakage; distributed load due to  
250 one floor housing of  $2.0 \text{ kNm}^{-2}$  (ABNT, 1980); height of the cutting slope (based on field data). In the case of the simulations  
251 that include leakage, one point of leaking constant value of  $1.0 \text{ m}^3\text{day}^{-1}$  was considered in the cut slope, after the 10<sup>th</sup> day of  
252 the simulation until the 35<sup>st</sup> day, since numerical experiments showed that a time interval of 10 days was adequate to  
253 minimize the effect of the uncertainties of initial pore-pressure conditions used in the simulations. It should be noted that this  
254 strategy helped to separate the effect of leakage from other anthropic factors, without impacting the results at the end of the  
255 simulation period (day 35).



256 For the transient flow analysis, the highest average moisture values of the three layers was considered (Landfill deposit -  
257  $\theta_{\text{mean}} = 33\%$ , Residual -  $\theta_{\text{mean}} = 31\%$ , Saprolite -  $\theta_{\text{mean}} = 34\%$ , to November 30, 2016 - light red region in Figure 9).  
258 Subsequently, the mean values of humidity were used to obtain the initial values of matrix suction from the representative  
259 water retention curves of each layer of the profile. The proper choice of the initial values of matrix suction is to provide the  
260 numerical model with a fast and coherent convergence in the pore-pressure distribution of water in the soil layers, aiming to  
261 adjust them satisfactorily to the rain data considered in the flow analysis (01 From December 1999 to January 4, 2000 - 35  
262 days).

263 For the transient flow analysis, the initial conditions of the simulations were derived assuming initial soil moisture values of  
264  $0.33 \text{ m}^3 \cdot \text{m}^{-3}$ ,  $0.31 \text{ m}^3 \cdot \text{m}^{-3}$  and  $0.34 \text{ m}^3 \cdot \text{m}^{-3}$ , for the landfill deposit, residual and saprolite layers respectively. These values  
265 correspond to average of the highest soil moisture values of the two probes during November 2016, and indicated by the  
266 light-red shaded area of Figure 9.

267 Subsequently, the mean moisture values were used to obtain the initial values of matrix suction from the representative water  
268 retention curves of each layer of the profile (Figure 8). This choice of the initial values of matrix suction of the numerical  
269 experiments proved to be crucial to achieve a fast and coherent convergence of pore-pressure distribution of soil layers in the  
270 simulations, since they are representative of the 35 days period considered in the flow analysis (From 01/12/1999 through  
271 04/01/2000). Based on this approach, the values of negative pore pressure (matrix suction) were -10 kPa for landfills, -40  
272 kPa for residual and -40 kPa for the saprolite.

273

### 274 3.4 Slope Safety Factor Analysis

275 Figure 10 shows the time variation of the slope safety factor (FS) during 35 days for the 2000 rainfall for the three profiles.  
276 In Figure 10, two "warning zones" are considered: zone of instability  $\text{FS} < 1.0$ , where ruptures should occur; and low stability  
277 ~~stable~~-zone,  $1.0 < \text{FS} < 1.5$ , which indicates a low possibility of landslide occurrence. In this warning zone the Brazilian  
278 Association of Technical Standards (ABNT, 1991) established the following conditions for the safety degree of the slope:  
279 High ( $1.3 \leq \text{FS} < 1.5$ ); Mean ( $1.15 \leq \text{FS} < 1.3$ ); Low ( $1.0 \leq \text{FS} < 1.15$ ).

280 For all three profiles analysed, it is clear that the effect of daily rain on the decrease of the FS (green line) was practically  
281 insignificant, with FS values above the 1.5 threshold (high safety degree of the slope); indicating very low likelihood of  
282 landslides. In the "rainfall only" scenario, the variations in FS values are due to the geotechnical and geomorphological  
283 characteristics of the analysed profiles only. For the "rainfall only" scenario, the difference between FS values in the three  
284 profiles are mainly due to: the surface slope, since the profile AA' is steeper than CC' which is steeper than BB'; due to  
285 differences in the thickness and location of the layers along the slope (Figure 4) and; the water table profile, related to the  
286 soil layers.

287 For the second scenario considered in the analysis of the stability, which includes cut-and-fill effects besides rainfall (red  
288 line in Figure 10), it was verified that the effect of terrain cuts caused minor effects in the slope safety factor. Except for the

289 case of the A-A' profile, which presents the FS condition  $<1.5$  between 32th and 35th day after the beginning of rainfall, FS  
290 values were above the 1.5 threshold. However, it is important to note that, in the case of the profile A-A', the decrease of FS  
291 was more pronounced than in the other profiles analysed, directly related to the positioning of the cuts considered along the  
292 slopes located based on field information. The configuration of the cuts used in this profile favour the wetting of the top soil  
293 layer and, consequently affected the whole profile stability.

294 The third scenario of Figure 10 (black line), where the joint influence of two anthropic factors (cut and leakage) with the  
295 rainfall of 2000 was considered, and the variations in FS values are significant. For the profile A-A', FS values remained  
296 below the threshold of 1.5; while in the other two profiles FS dropped below 1.5 between the 32nd and 35th days of  
297 simulations in the case of the B-B' profile, and on day 17th for the C-C' profile. It should be noted that, after the 11th after  
298 the beginning of simulation, FS values become sensitive to rainfall variability.

299 In addition, it can be seen in Figure 10 that the profiles B-B' and C-C' showed greater sensitivity to leakages, mainly due to  
300 the geological-geotechnical characteristics, and the location of the cuts along the slopes, that favoured the decrease of the  
301 matrix suction values and, therefore, induced instability in both profiles. In addition, critical condition,  $FS < 1.0$ , in profiles  
302 A-A' and C-C' are verified between days 32nd and 35th after the beginning of simulations, in response to the significant  
303 rainfall that occurred at the period. However, it is observed that, under the influence of leakage, previous rainfall history  
304 played a role since the factor of stability is lower previously to the large rainfall event of the end of the simulation period.  
305 This can be seen in more clearly in the profile B-B' of Figure 10: in the dry period between day 15 and day 22 after the  
306 beginning of simulation, it is verified a quick recovery of stability in the simulations that includes the effect of leakage  
307 (black curve), which is interrupted with the return of the rainfall.

308 Finally, in the fourth scenario of Figure 10 (light brown line), when all the anthropic factors (cut, leakage and housing loads)  
309 are considered together with the daily rainfall. For most of the time, FS values remained below the threshold of 1.5 in in the  
310 A-A' and B-B' profiles, while in the case of the profile C-C' only after the day 34th of the simulation. The probability of  
311 landslides increased significantly ( $FS < 1.0$ ) in all profiles from day 32 of the simulation in response to heavy rainfall at the  
312 end of the period. In the case of the profile C-C' (light brown line), the inclusion of housing loads appears to provide more  
313 stability to the profile, probably related to the fact that the critical failure surface estimated by the numerical model was  
314 different from that assumed in the case scenario 3 (black line).

315 Based on the assessment of the slope safety factor presented in Figure 10, it is clear that the probability of landslides  
316 associated to 2000 rainfall on slopes covered with natural vegetation is very low. When considering the influence of rainfall  
317 in conjunction with anthropogenic factors, there was a significant decrease in the safety factors in all the profile studied,  
318 although the effect varied between slopes depending on the geological-geotechnical profile characteristics, geomorphological  
319 conditions, water table position and the anthropic conditions, thus is, the positioning of cuts, leakage and housing loads along  
320 the slope.

321 In general, slopes became unstable ( $FS < 1.0$ ) between 32nd and 35th after the beginning of simulations when high daily  
322 accumulated values were verified. Since most of the landslide occurred on day 32nd, it follows that the model successfully

323 predicted the time were the landslides began. However, it should be noted that previous accumulated rainfall values were  
324 crucial to create favourable conditions for triggering landslides as shown by Figure 10 after the 30th day from the beginning  
325 of simulation.

326 Santoro et al. (2010) recommended in-situ technical surveys of urban hazardous areas after accumulated 72-hour rainfall  
327 equal to 60, 80 and 100 mm (depending on the municipality), in order to identify evidences of the imminence of landslides  
328 and to enforce eventual preventive removal of population. It can be seen in Figure 10 that the 72h accumulated rainfall were  
329 35 mm for the day 30 after the beginning of simulation; 35 mm for the day 31; 60 mm for the day 32; 191 mm for the day  
330 33. Thus, critical rainfall thresholds (60-100 mm) were exceeded between 32nd and 33th day for the events recorded in the  
331 year 2000.

332 In this period, the FS in the three analyzed profiles presented the lowest values, located exactly between the "low-medium  
333 security zone" ( $1.0 < FS < 1.3$ ) and "unstable zone" ( $FS < 1.0$ ), which shows that the "anthropic and natural factors integrated  
334 analysis method" proposed in this paper successfully predicted the beginning of landslides. Although the 72h rainfall  
335 threshold value proposed by Santoro et al (2010) proved to be valid for the 2000 event, results of the simulation indicated  
336 that the rainfall 30 days previous to the landslides was crucial to bring FS values closer to critical levels, indicating that  
337 critical value presents limitations on slopes initially drier.

#### 338 **4 Conclusions**

339 The Geo-slope model proved to be an efficient and useful tool to predict the landslide of Campos do Jordão municipality due  
340 to the rainfall event of 2000 and allowed to disentangle the effects of cut-and-fill, construction practices and pipe leakage in  
341 three representative slopes of the area. The use of numerical models that perform flow and stability analyses considering the  
342 simultaneous influence of natural and anthropic variables showed to be accurate for the prediction of occurrences of  
343 landslides on urban slopes.

344 Regarding the rainfall critical values use in early warning system by CEMADEN and the Civil Defense for the Campos do  
345 Jordão Municipality, although adequate for the event of 2000, our study show that the previous rainfall history, in  
346 combination with leakages, played a fundamental role to create favorable conditions for the occurrence of landslides. This is  
347 related to the fact that leakages contribute to keep the soil profile closer to saturation at the beginning of the period of more  
348 intense rainfall, and consequently the developing of positive pore-pressure conditions. In other words, the threshold currently  
349 used for issue early warning would result in late alarms under initial drier soil conditions, at least in heavily disturbed  
350 landscapes.

351 The results of the stability analyses confirmed the hypothesis that the occurrence of landslides in the study area cannot be  
352 attributed solely and exclusively to the rainfall events of the year 2000, despite the significant accumulated values.  
353 Therefore, numerical modelling results corroborated the fact that the occurrence of landslides was the combination of natural  
354 and anthropic factors, with the decisive influence of the latter, thus is, due to the presence of several cuts along the slope  
355 combined with load of constructions and leakage. Clearly, human interventions on natural slopes play a fundamental role in

356 triggering landslides in heavily populated steep slopes surrounding urban areas. Once shallow landslides in the study area  
357 usually occur in cut and fill slopes, the rupture surface size and the amount of material mobilized do not vary significantly  
358 among events. Therefore, the most useful information for an early warning system perspective is to know whether the value  
359 of FS is below 1.0, regardless how much below that threshold the slope safety factor is. Another relevant information is the  
360 timing of the landslide events, since such information is crucial to determine the rainfall thresholds for issuing an early  
361 warning. Therefore, information about the rupture surface size, which is essential for assessing potential damages, is beyond  
362 the scope of this study.

363 Considering that the pattern of land use and construction used in the simulations is representative of most of the  
364 neighborhood of Brazilian urban areas, the methodology used in this paper needs to be repeated and verified in other areas in  
365 order to establish more accurate critical threshold that trigger landslides. Moreover, since the prone to landslide areas of  
366 Campos do Jordão Municipality are not the most populated of Brazil compared, for instance, to the outskirts of several  
367 metropolitan areas, it becomes crucial to verify whether a mosaic of site-specific rainfall thresholds is needed in heavily  
368 occupied areas, rather a single regional threshold, as suggested by Segoni et al. (2014). In this context, this study  
369 demonstrated the using the slope safety factor is viable for determine more accurate rainfall threshold that trigger landslides,  
370 with direct impacts on the credibility of early warning systems, which relies in minimizing false alarms or premature/late  
371 warnings.

372 Although the results of this study have uncertainties mainly associated with the geotechnical parameters used in the flow  
373 analysis and slope stability, it is the first comprehensive analysis of the factors responsible for triggering landslide in Brazil  
374 that integrates field evidence, anthropic effects, geotechnical data and numerical simulation. Since simulations results  
375 indicated that the slope safety factor FS was sensitive to both geotechnical and anthropic factors, future studies of slope  
376 stability probabilistic analysis, which takes into account the wider range of parameters values that occur in the study area, are  
377 needed.

378 Finally, considering that this work have demonstrated that the anthropic factors are the main instability factors in urban  
379 slopes, it is essential that urban managers and planners promote public policies and enforce laws that restrict the occupation  
380 of landslide susceptible areas. Detailed surveys to identify prone to landslide areas are essential, since many urban areas of  
381 Brazil lack zoning of hazardous areas, which is essential to implement regulations. Besides this, educational campaigns  
382 regarding the adoption of better construction practices and reducing piping leakage will be helpful in already consolidated  
383 occupied areas.

390 **References**

- 391 ABNT - Brazilian Association of Technical Standards: Determination of the specific mass, NBR-6508. Rio de Janeiro, 8p,  
392 1984a.
- 393 ABNT - Brazilian Association of Technical Standards: Loads for the buildings structures calculation, NBR 6120. Rio de  
394 Janeiro, 5p, 1980.
- 395 ABNT - Brazilian Association of Technical Standards: Rocks and soils – terminology, NBR-6502. Rio de Janeiro, 1995.
- 396 ABNT - Brazilian Association of Technical Standards: Slopes stability, NBR-11682. Rio de Janeiro, 39p, 1991.
- 397 ABNT - Brazilian Association of Technical Standards: Soil – determination of the liquid limit, NBR 6459. Rio de Janeiro,  
398 6p, 1984c.
- 399 ABNT - Brazilian Association of Technical Standards: Soil – determination of the plastic limit, NBR 7180. Rio de Janeiro,  
400 3p, 1984d.
- 401 ABNT - Brazilian Association of Technical Standards: Soil – grain size analysis test, NBR-7181. Rio de Janeiro, 13p,  
402 1984b.
- 403 Acharya, K. P., Bhandary, N. P., Dahal, R. K., Yatabe, R.: Seepage and slope stability modelling of rainfall-induced slope  
404 failures in topographic hollows, *Geomatics, Natural Hazards and Risk*, 7(2), 721-746, 2016.
- 405 Ahrendt, A. and Zuquette, L. V.: Triggering factors of landslides in Campos do Jordão City, Brazil, *Bulletin of Engineering  
406 Geology and the Environment*, 62, 231-244, 2003.
- 407 Ahrendt, A.: Gravitational mass movements - proposal of a forecast system: application at the urban area of Campos do  
408 Jordão City-SP, Brazil. (In Portuguese), Doctoral thesis, School of Engineering of São Carlos, São Paulo University, Brazil,  
409 390 pp., 2005.
- 410 Almeida, F F M. 1976. The system of continental rifts bordering the Santos Basin, Brazil. In: *Anais Academia Brasileira de  
411 Ciências, CONTINENTAL MARGINS OF ATLANTIC TYPE*, São Paulo, 1975, 48 (Suplemento): 15-26.
- 412 Andrade, E.: Risk mapping associated to landslides, flood, erosion and undercutting of riverbank in municipality of Campos  
413 do Jordão, São Paulo State, Brazil (in Portuguese), IG-CEDEC Technical Report number 01/2013, 4, 2014.
- 414 Baum, R. L., Savage, W. Z., and Godt, J. W.: TRIGRS – a FORTRAN program for transient rainfall infiltration and grid-  
415 based regional slope stability analysis, *US Geological Survey Open File Report 2002-424*, 38 pp, 2002.
- 416 Beven, K. J. and Kirkby, M. J.: A physically based variable contributing area model of basin hydrology, *Hydrological  
417 Sciences Bulletin*, 24(1), 43-69, 1979.
- 418 Burton, A. and Bathurst, J.: Physically based modelling of shallow landslide sediment yield at a catchment scale,  
419 *Environmental Geology*, 35, 89–99, 1998.
- 420 Campbell Scientific: EnviroSCAN™ soil water content profile probes, Instruction Manual, 48p, “available at:  
421 <https://s.campbellsci.com/documents/us/manuals/envirosmart.pdf>, 2016.”

422 CEDEC – Civil Defense Coordination of the São Paulo State: databases of the summer operation emergency calls from 2000  
423 through 2013 (in Portuguese), São Paulo, 2013.

424 CEPED - Centro Universitário de Estudos e Pesquisas sobre Desastres. Atlas Brasileiro de Desastres Naturais 1991 – 2010:  
425 volume Brasil. Florianópolis: UFSC, 2012. 127p.

426 Cho, S. E.: Infiltration analysis to evaluate the surficial stability of two-layered slopes considering rainfall characteristics,  
427 *Engineering Geology*, 105, 32-43, 2009.

428 Coelho Netto, A. L., Avelar, A. S., Vianna, L. G. G., Araújo, I. S., Ferreira, D. L. C., Lima, P. H. M., Silva, A. P. A., and  
429 Silva, R. P.: The extreme landslide disaster in Brazil, *Landslide Science and Practice*, 6, 377-384, 2013.

430 Costa Filho, L. M. and Campos, T. M. P.: Anisotropy of a gneissic residual soil, in: *Proceedings of the 9th Pan-American  
431 Conference on Soil Mechanics and Foundations Engineering*, Vina Del Mar, Chile, 51-61, 1991.

432 Crosta, G.: Regionalization of rainfall thresholds: an aid to landslide hazard evaluation, *Environ Geol.*, 35, 131-145, 1998.

433 D’Orsi, R., D’Ávila, C., Ortigão, J. A. R., Dias, A., Moraes, L., and Santos, M. D.: Rio-Watch: The Rio de Janeiro Landslide  
434 Watch System, in: *Proceedings of the 2<sup>nd</sup> Pan-American Symposium on Landslides*, Rio de Janeiro, Brazil, 21-30, 1997.

435 define a mosaic of triggering thresholds for regional-scale warning systems, *Nat. Hazards Earth Syst. Sci.*, 14, 2637–2648,

436 Dietrich, W. E., Asua, R. R., Orr, J. C. B., and Trso, M.: A validation study of the shallow slope stability model,  
437 SHALSTAB, in the forest lands of Northern California. *Stillwater Ecosystem, Watershed and Riverine Sciences*, Berkeley,  
438 59 pp, 1998.

439 Frattini, P.; Crosta, G., and Sosio, R.: Approaches for defining thresholds and return periods for rainfall-triggered shallow  
440 landslides, *Hydrol Process.*, 23, 1444-1460, 2009.

441 Gasmó, J. M.; Rahardjo, H., and Leong, E. C.: Infiltration effects on stability of a residual soil slope, *Computers and  
442 Geotechnics*, 26, 145-65, 2000.

443 Geo-Slope: Seepage modeling with SEEP/W: an engineering methodology, User manual, Geo-Slope International, 199p,  
444 2012b.

445 Geo-Slope: Stability modeling with SLOPE/W: an engineering methodology, User manual, Geo-Slope International, 238p,  
446 2012a.

447 GeoStudio: GeoStudio Tutorials includes student edition lessons. Calgary, Alberta, Canadian: Geo-Slope International Ltd.,  
448 2012.

449 Guzzetti, F.; Peruccacci, S.; Rossi, M., and Stark, C.P.: Rainfall thresholds for the initiation of landslides in central and  
450 southern Europe, *Meteorology and Atmospheric Physics*, 98, 239-267, 2007.

451 Huat, B .B. K., Ali, F. H., and Rajoo, R. S. K.: Stability analysis and stability chart for unsaturated residual soil slope,  
452 *American Journal of Environmental Sciences*, 2 (4), 154-160, 2006.

453 IBGE – Brazilian Institute of Geography and Statistics, social and economic data of the Brazilian citizens (in Portuguese),  
454 “available at: <http://cidades.ibge.gov.br/painel>, 2016.”

455 Iverson, R. M.: Landslide triggering by rain infiltration, *Water Resour. Res.*, 36, 1897-1910, 2000.

456 Kim, J., Jeong, S., Park, S., and Sharma, J.: Influence of rainfall-induced wetting on the stability of slopes in weathered soils,  
457 *Engineering Geology* ,75, 251-262, 2004.

458 Lagomarsino, D., Segoni, S., Fanti, R., and Catani, F.: Updating and tuning a regional-scale landslide early warning system,  
459 *Landslides*, 10, 91–97, 2013. DOI: 10.1007/s10346-012-0376-y

460 Liao Z, Hong Y, Wang J, Fukuoka H, Sassa K, Karnawati D, Fathani F. (2010) Prototyping an experimental early warning  
461 system for rainfall-induced landslides in Indonesia using satellite remote sensing and geospatial datasets. *Landslides* 7:317–  
462 324.doi:10.1007/s10346-010-0219-7.

463 Londe, L. R., Coutinho, M. P., Di Gregório, L. T., Santos, L. B. L., and Soriano, E.: Water related disasters in Brazil:  
464 perspectives and recommendations (in Portuguese), *Ambiente and Sociedade*, 17(4), 133-152, 2014.

465 Marinho, F. A. M., Oliveira, O. M.: The filter paper method revisited. *Geotechnical Testing Journal*, ASTM, 29(3):250-258,  
466 2006

467 Modenesi-Gauttieri, MC; Hiruma, ST. 2004. A Expansão Urbana no planalto de Campos do Jordão. Diagnóstico  
468 geomorfológico para fins de planejamento. *Revista do Instituto Geológico, São Paulo*, 25(1/2), 1-28, 2004.

469 Montrasio L (2000) Stability analysis of soil slip. In: Brebbia CA (ed) *Proceedings of International Conference BRisk 2000*^.  
470 Wit Press, Southampton, pp 357–366

471 Montrasio L, Valentino R (2008) A model for triggering mechanisms of shallow landslides. *Nat Hazards Earth Syst Sci*  
472 8:1149–1159. doi:10.5194/nhess-8-1149-2008

473 Montrasio L, Valentino R, Losi GL (2011) Towards a real-time susceptibility assessment of rainfall-induced shallow  
474 landslides on a regional scale. *Nat Hazards Earth Syst Sci* 11:1927–1947. doi:10.5194/nhess-11-1927-2011.

475 Ng, C.W.W. and Shi, Q.: Influence of rainfall intensity and duration on slope stability in unsaturated soils, *Quarterly Journal*  
476 *of Engineering Geology*, 31, 105-113, 1998.

477 Ogura, AT; Silva, FC; Vieira, AJNL. Zoneamento de risco de escorregamento das encostas ocupadas por vilas  
478 operárias como subsídio à elaboração do plano de gerenciamento de áreas de risco da estância climática de Campos do  
479 Jordão - SP. 2004. In: *Simpósio Brasileiro de Desastres Naturais, 1º, 2004, Florianópolis. Anais... Florianópolis:*  
480 *GEDN/UFSC, 2004. p. 44-58. (CD-ROM).*

481 Oh, W.T. and Vanapalli, S.K.: Influence of rain infiltration on the stability of compacted soil slopes, *Computers and*  
482 *Geotechnics*, 37, 649-657, 2010.

483 Pack RT, Tarboton DG, Goodwin CN (1998) SINMAP—a stability index approach to terrain stability hazard mapping.  
484 *User’s manual. Terratech Consulting Ltd, Salmon Arm.*

485 Pack, R. T., Tarboton, D. G., and Goodwin, C. N.: The SINMAP approach to terrain stability mapping, in: *Proceedings of*  
486 *the 8th Congress of the International Association of Engineering Geology, Vancouver, Canada, 21-25, 1998.*

487 Rahardjo, H., Ong, T. H., Rezaur, R. B., and Leong, E. C.: Factors controlling instability of homogeneous soil slopes under  
488 rainfall, *J. Geotech. Geoenviron. Eng.*, 133 (12), 1532-1543, 2007.

489 Reis, R.M., Azevedo, R.F., Botelho, B.S., and Vilar, O.M.: Performance of a cubical triaxial apparatus for testing saturated  
490 and unsaturated soils, *Geotechnical Testing Journal*, 34 (3), 1-9, 2011.

491 Ridente, J. L., Ogura, A. T., Macedo, E. S., Diniz, N. C., Alberto, M. C., and Santos, H. P.: Accidents associated to mass  
492 movements that were occurred in municipality of Campos do Jordão, SP, at January 2000: technical actions after the  
493 disasters (in Portuguese), IPT publications number 2815, 14p, 2002.

494 Rigon, R., Bertoldi, G., Over, T. M.: Geotop: a distributed hydrological model with coupled water and energy budgets,  
495 *Journal of Hydrometeorology*, 7(3), 371– 388, 2006.

496 Rossi G, Catani F, Leoni L, Segoni S, Tofani V. (2013). HIRESSS: a physically based slope stability simulator for HPC  
497 applications. *Nat. Hazards Earth Syst Sci* 13:151–166. doi:10.5194/nhess-13-151-2013.

498 SABESP: Leak tests, <http://site.sabesp.com.br/site/interna/Default.aspx?secaoId=244>, Accessed 04 Abril 2016, 2016.

499 SABESP: Water reduction program not charged, Synthetic report, Sao Paulo: Lyonnaise des Eaux Services Associés –  
500 LYSA, 1993.

501 Santoro, J., Mendes, R. M., Pressinotti, M. M. N. and Manoel, G. R.: Correlation between rainfall and landslides occurred  
502 during the operation of the prevention plan of civil defense in State of São Paulo, SP (in Portuguese), in: Proceedings of the  
503 7th Brazilian Symposium on Geotechnical and Geoenvironmental Cartography, Maringá, Paraná, 1-15, 2010.

504 [Segoni, S., Rosi, A., Rossi, G., Catani, F., and Casagli, N.: Analysing the relationship between rainfalls and landslides to  
505 define a mosaic of triggering thresholds for regional-scale warning systems. \*Nat. Hazards Earth Syst. Sci.\*, 14, 2637-2648,  
506 2014. doi:10.5194/nhess-14-2637-2014](#)

507 Tatizana, C., Ogura, A. T., Cerri, L. E. S., and Rocha, M. C. M.: Numerical modeling of the analysis of correlation between  
508 rainfall and landslides applied to the slopes of the Serra do Mar in municipality of Cubatão (in Portuguese), in: Proceedings  
509 of the 2nd Brazilian Congress of Engineering Geology, 237-248, 1987.

510 Terlien, M. T.: The determination of statistical and deterministic hydrological landslide triggering thresholds, *Environ Geol.*,  
511 35, 124-130, 1998.

512 Thiebes B, Bell R, Glade T, Jäger S, Mayer J, Anderson M, Holcombe L.(2014). Integration of a limit-equilibrium model  
513 into a landslide early warning system. *Landslides* 11:859–875. doi:10.1007/s10346-013-0416-2.

514 Tofani, V., Dapporto, S., Vannocci, P., and Casagli, N. (2006). Infiltration, seepage and slope instability mechanisms during  
515 the 20–21 November 2000 rainstorm in Tuscany, central Italy, *Nat. Hazards Earth Syst. Sci.*, 6, 1025–1033,  
516 doi:10.5194/nhess-6-1025-2006.

517 Van Asch, T. W. J., Buma, J., and Van Beek, L. P. H.: A view on some hydrological triggering systems in landslides,  
518 *Geomorphology*, 30, 25-32, 1999.

519 Van Genuchten, M. T.: A closed-form equation for predicting the hydraulic conductivity of unsaturated soils, *Journal of the*  
520 *Soil Science Society of America*, 44, 892-898, 1980.

**Formatado:** Cor da fonte: Vermelho



523

524

Table 1 – Historical disasters in Campos do Jordão Municipality. Source: Ridente et al. (2002) and Andrade (2014).

Process	Location	Year	Damages	Causes
Earthflow	Vila Albertina	1972	17 fatalities 60 houses buried	Saturated soil (8m thick), loading and vibration due to construction activities
Landslide	Britador, Vila Santo Antonio and Vila Paulista Popular	1991	149 affected 11 houses buried 4 injured	214.5 mm of rainfall in three days
Landslide and Mudflow	Britador, Vila Albertina, Vila Santo Antônio, Vila Nadir Vila Sodipe and Vila Paulista Popular	2000	10 fatalities 1840 affected	453.2 mm in five days

525

526

527

Table 2 – Results of the geotechnical survey of soils of the study areas.

Sample	Depth (m)	Soil layer	USCS	Unit weight (kN/m <sup>3</sup> )	Effective cohesion (kPa)	Effective friction angle (°)	Hydraulic conduct. (m/s)	Gravel (%)	Sand (%)	Silt (%)	Clay (%)	w <sub>L</sub> (%)	w <sub>p</sub> (%)	IP (%)
SD-01	2.0	R	SC	18.3	37	56	4.44 e <sup>-6</sup>	10	53	25	12	27	18	9
	4.6	S	SC	19.1	18	37	9.46 e <sup>-6</sup>	0	53	35	12	35	22	13
	6.6	S	SC	17.9	2	49	7.93 e <sup>-6</sup>	0	59	27	14	29	20	9
SD-02	2.6	S	SC	21.4	19	34	1.18 e <sup>-6</sup>	5	50	21	24	28	17	11
	4.6	S	SM	17.5	14	42	3.76 e <sup>-6</sup>	0	73	14	13	33	20	13
SD-03	1.6	S	SM-SC	18.1	22	43	5.25 e <sup>-6</sup>	1	59	29	11	22	15	7
	2.6	S	SM-SC	16.8	2	52	6.13 e <sup>-7</sup>	5	55	30	10	23	17	6
SD-05	12.8	S	SC	17.5	48	54	2.77 e <sup>-7</sup>	0	55	33	12	32	21	11
SD-06	7.6	S	SM	17.8	42	28	3.09 e <sup>-6</sup>	1	72	15	12	-	-	-
Block-1	2.0	S	SM	16.0	2	53	9.37 e <sup>-7</sup>	0	72	21	7	-	-	-
Block-2	2.0	S	SM	16.0	49	37	2.98 e <sup>-6</sup>	0	55	42	3	-	-	-
Block-3	3.0	S	SM	16.0	13	46	4.44 e <sup>-6</sup>	0	58	28	14	-	-	-

528

# Residual soil (R); Saprolite (S).

529

530

531

532

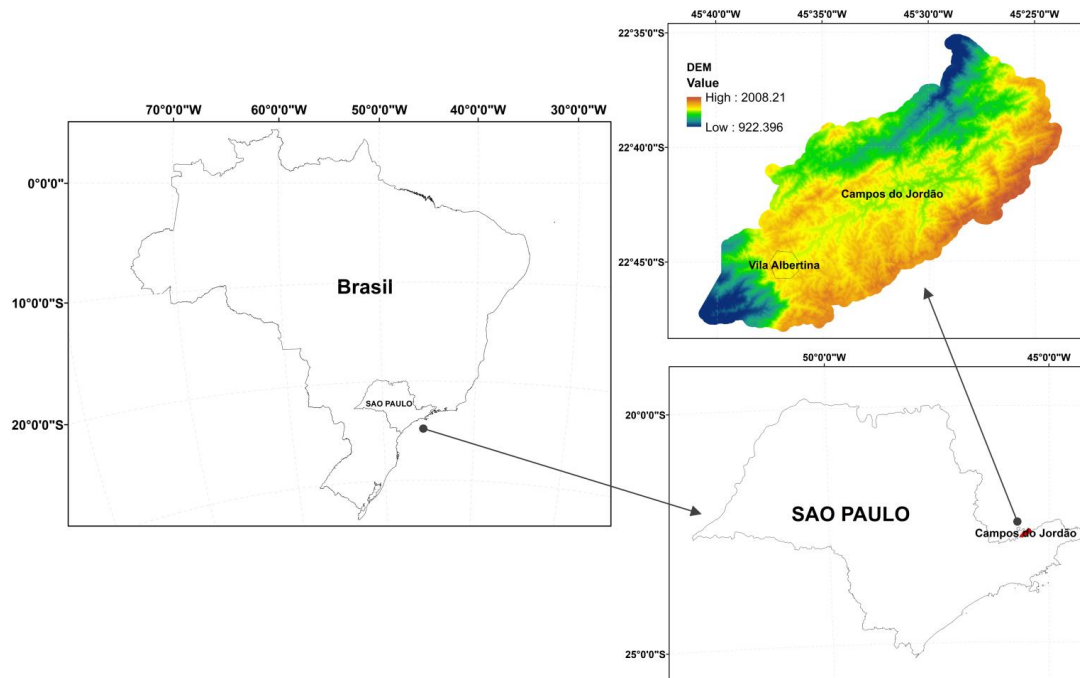
533  
534

Table 3 – Geotechnical and anthropic parameters used on unsaturated seepage and stability analysis

Profile	Slope declivity (°)	Slope height (m)	Geotechnical					Anthropic				
			Soil layers	Shear strength effective parameters#	Unit weight (kN/m <sup>3</sup> )#	Rainfall (m/day)	Ksat (m/s)	Pore water pressure (kPa)	Level of the water table	Load in the slope (kN/m <sup>2</sup> )	Height of the cut slope (m)	Leaking in the slope (m <sup>3</sup> /day)
A - A'	11 - 40	130										
			Fill Deposit	c' = 2 kPa φ' = 31°	14,9	Rainfall events of the 2000 year	9.50 e <sup>-6</sup>	-7				
B - B'	16 - 33	95	Residual	c' = 15 kPa φ' = 36°	18,3		4.44 e <sup>-6</sup>	-40	Data of SPT	2.0	6.0	1.0
			Saprolite	c' = 21 kPa φ' = 43°	19,1		5.43 e <sup>-6</sup>	-40				
C - C'	15 - 35	87										

# Fill Deposit (geotechnical parameters from Ahrendt, 2005)

535  
536  
537  
538  
539  
540  
541  
542  
543  
544  
545  
546  
547  
548  
549  
550  
551  
552  
553  
554



**Figure 1.** Geographical location of Campos do Jordão municipality and an inset of the study site.

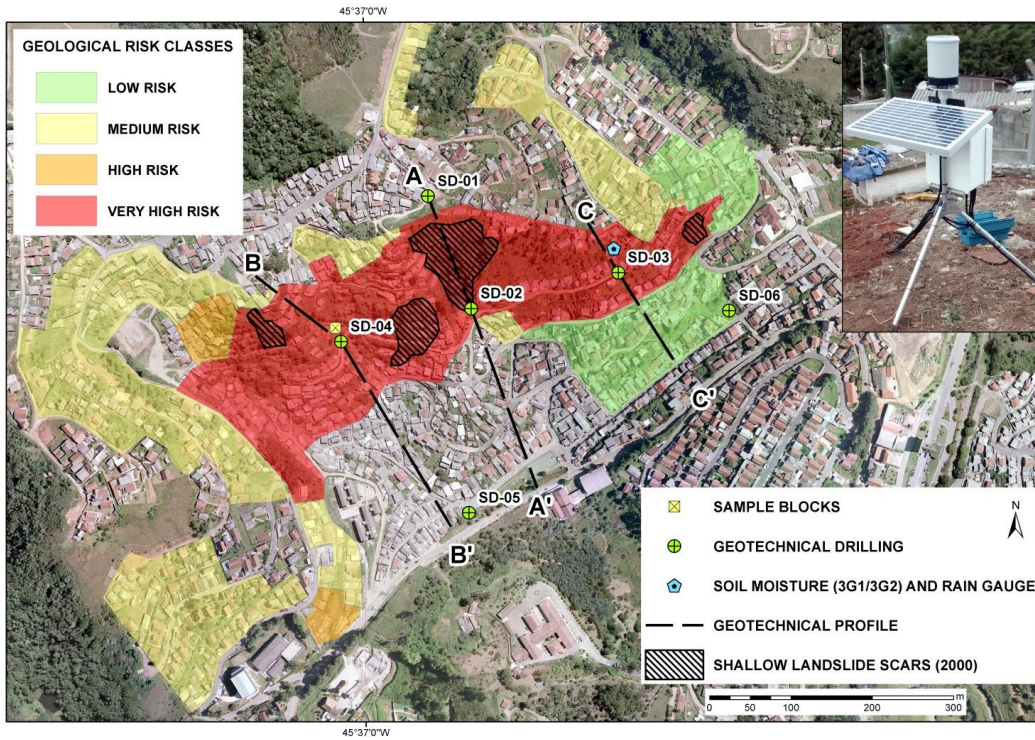
555  
 556  
 557  
 558  
 559  
 560  
 561  
 562  
 563  
 564  
 565  
 566  
 567  
 568  
 569

570  
571



**Figure 2.** Shallow landslides that happened in 2000 on the study site (Source: Ridente et al., 2002).

572  
573  
574  
575  
576  
577  
578  
579  
580  
581  
582  
583



585  
 586 **Figure 3.** Satellite image of the study site showing the location of monitoring instruments (symbols), geotechnical transects (dotted lines  
 587 along the slopes); landslide susceptibility areas indicating the level of risk (areas shaded in yellow, orange and red); scars of previous  
 588 shallow landslides (black cross-hatched area).

589

590

591

592

593

594

595

596

597

598

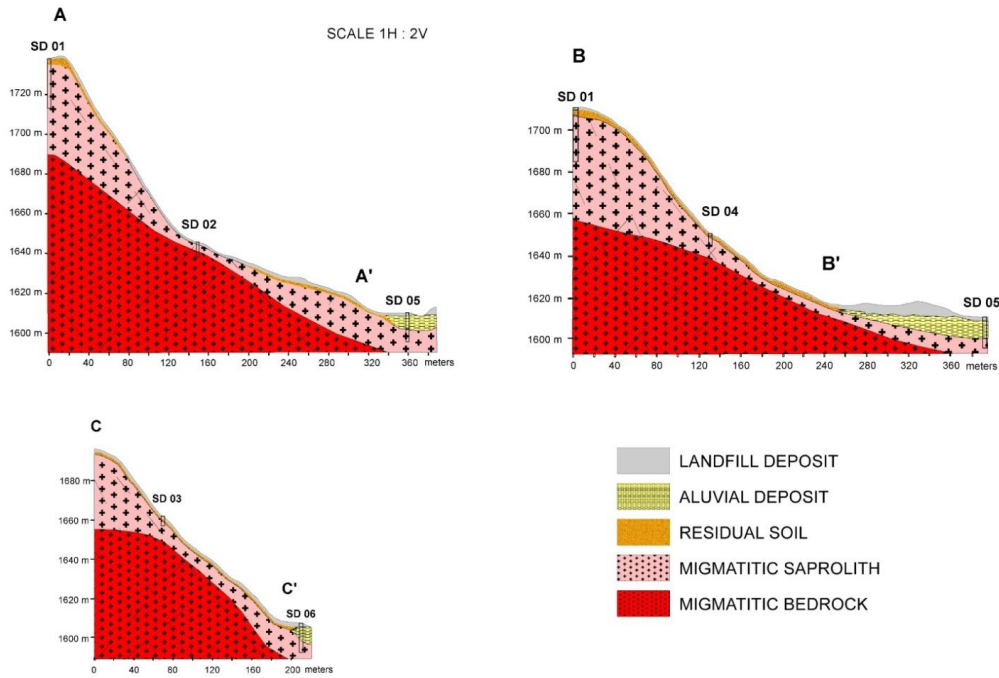


**Figure 4.** Geological-geotechnical profiles of the study area derived from the geotechnical survey.

600  
601  
602  
603  
604  
605  
606  
607  
608  
609  
610  
611  
612  
613  
614  
615  
616

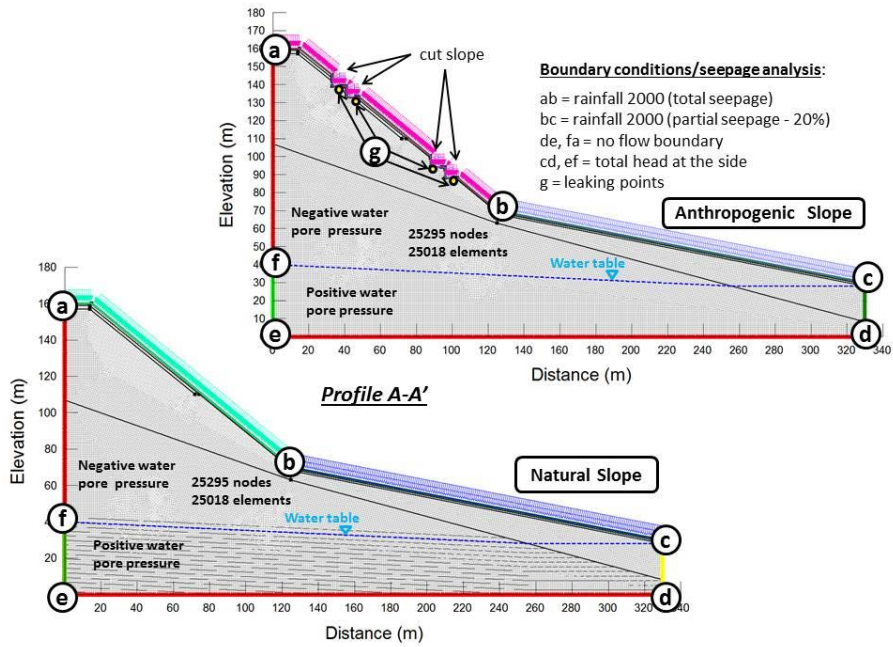


**Figure 5.** Slope geometry and boundary conditions used in the unsaturated transient seepage analysis considering natural and anthropogenic factors (rainfall, cut slope and leakage).

618  
 619  
 620  
 621  
 622  
 623  
 624  
 625  
 626  
 627  
 628  
 629  
 630  
 631  
 632  
 633

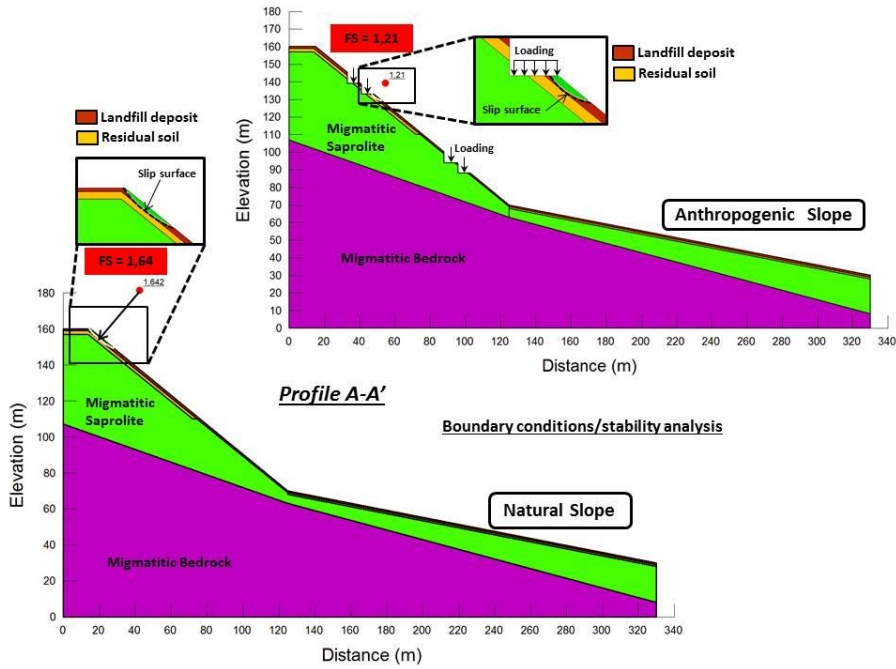
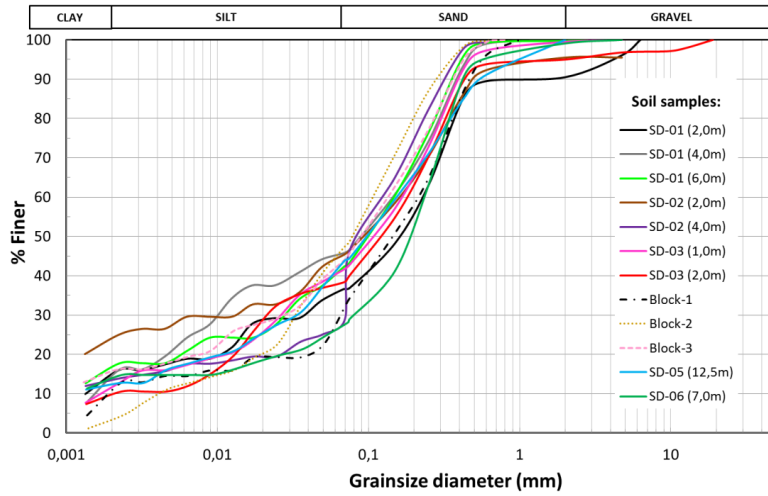


Figure 6. Slope geometry and boundary conditions used in the stability analysis considering natural and anthropogenic factors (rainfall, cut slope, loading and leakage).



651



652

653

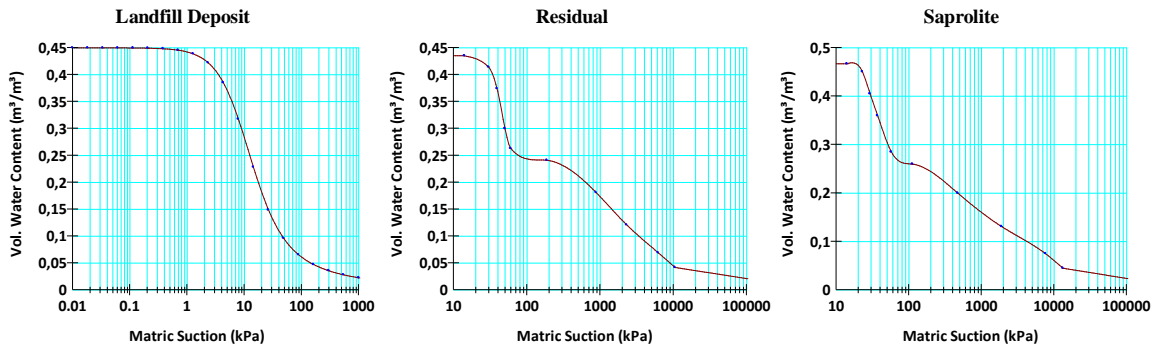
654

655

656

657

Figure 7. Granulometric distribution for the residual soil and the saprolite of the six boreholes analysed (SD-01 to SD-06) and for the undisturbed soil cores (Block-1 to Block-3).



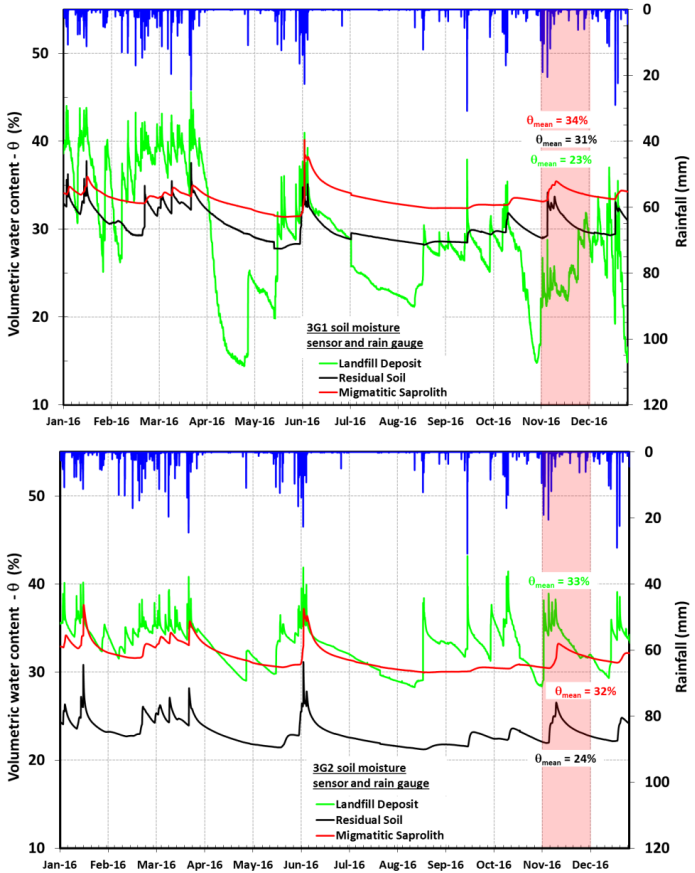
658

659

660

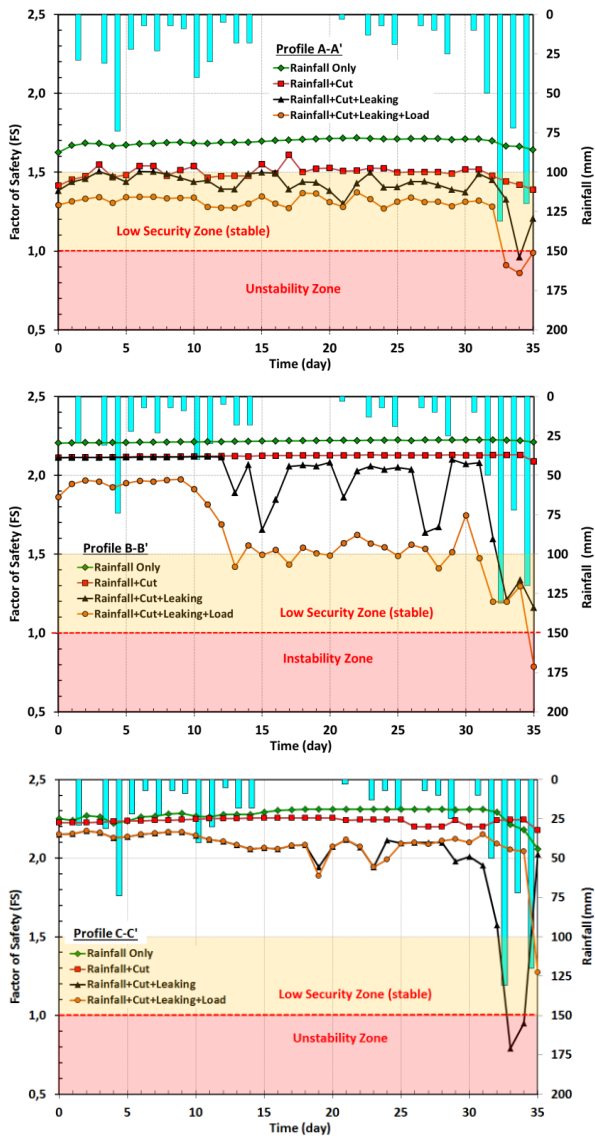
661

Figure 8. Water retention curves of the three soil types used in transient seepage analysis.



663  
664  
665  
666  
667  
668  
669  
670  
671

**Figure 9.** Time variation of soil moisture at different depths during 2016 in the study area in the sensor 3G1 (upper graph) and 3G2 (bottom graph).



**Figure 10.** Time variation of the slope safety factor for natural conditions and taken into account the additional effects introduced by anthropic disturbances on profiles A-A', B-B' and C-C'.

672  
673  
674